



## Dielectric properties of chitosan and two ionic derivatives: Effect of counter anions

Ahmed Salama, Fathia Mohamed, Peter Hesemann

### ► To cite this version:

Ahmed Salama, Fathia Mohamed, Peter Hesemann. Dielectric properties of chitosan and two ionic derivatives: Effect of counter anions. Carbohydrate Polymers, 2022, 297, pp.120018. 10.1016/j.carbpol.2022.120018 . hal-03795784

**HAL Id: hal-03795784**

**<https://cnrs.hal.science/hal-03795784>**

Submitted on 4 Oct 2022

**HAL** is a multi-disciplinary open access archive for the deposit and dissemination of scientific research documents, whether they are published or not. The documents may come from teaching and research institutions in France or abroad, or from public or private research centers.

L'archive ouverte pluridisciplinaire **HAL**, est destinée au dépôt et à la diffusion de documents scientifiques de niveau recherche, publiés ou non, émanant des établissements d'enseignement et de recherche français ou étrangers, des laboratoires publics ou privés.

**Dielectric properties of chitosan and two ionic derivatives: Effect of counter anions**

Ahmed Salama<sup>1,2, \*</sup>, Fathia Mohamed<sup>3</sup> and Peter Hesemann<sup>1</sup>

<sup>1</sup> Cellulose and Paper Department, National Research Centre, 33 El-Behouth St., Dokki, P.O. 12622, Giza, Egypt

<sup>2</sup> Institut Charles Gerhardt de Montpellier, UMR CNRS 5253 Université de Montpellier-CNRS-ENSCM, Campus CNRS, 1919 route de Mende, 34293 Montpellier Cedex 05, France

<sup>3</sup> Spectroscopy Department, Physics Research institute, National Research Centre, 33 El-Bohouth St., 12622, Dokki, Giza, Egypt

\*Corresponding author: ahmed\_nigm78@yahoo.com

**Keywords:** Chitosan; Cationic derivative; Dielectric relaxation; Conductivity

**Abstract**

We report herein the dielectric properties response of two ionic chitosan derivatives. More specifically, we report here chitosan derivatives bearing guanidinium groups, prepared through the reaction between chitosan and cyanamide when scandium (III) triflate is present. The anionic counter ions of the guanidinium groups could be changed by working either in acetic acid or hydrochloric acid. In this way, two chitosan derivatives, namely N-guanidinium chitosan acetate (GChAc) and N-guanidinium chitosan chloride (GChCl), were produced. The materials were investigated by <sup>13</sup>C solid state NMR, FT-IR spectroscopy, SEM and TEM analysis and compared with the parent chitosan. The relaxation behavior of parent chitosan and new chitosan derivatives has been investigated by dielectric spectroscopy over wide temperature and frequency ranges, indicating that local motion is affected by counter ions. Due to these features, these materials are interesting candidates as high-power electrical materials for green technological applications.

## 1. Introduction

Due to the growing demand for energy and the reduction of fossil fuels, scientists have been exploring alternative and more sustainable sources of energy. In this context, supercapacitors are currently attracting growing interest due to their high-power density and ability to charge quickly without causing any damage such as explosion or thermal runaway. Today, electrodes and electrolytes used in supercapacitors contain non-renewable and hazardous materials such as metal oxides and synthetic polymers, which are often harmful to the environment. The use of polysaccharides could potentially be an alternative to these materials. Polysaccharides such as cellulose are among the most ancient electrically insulating materials used in cables (Le Bras et al., 2015). Alternative biomass materials have attracted significant attention as innovative solutions in the field of novel high-performance film dielectric capacitor (Salama & Hesemann, 2020a; Yin et al., 2020).

Chitin is one of the most abundant natural polymers. It can be found in the exoskeleton of crustaceans, mollusks, insects, and other invertebrates as well as in the cells of fungi and moulds. Chitin is insoluble in all conventional solvents. However, partially deacetylated chitin, *i.e.* chitosan (Ch), is well soluble in weakly acidic media, e.g. in acetic acid (Salama et al., 2017). Under these conditions, the amino groups of chitosan undergo protonation, thus forming a polyelectrolyte with cationic charges on the chitosan backbone (Salama & El-Sakhawy, 2014). Chitosan,  $\beta$ -(1,4)-linked D-glucosamine, attracted huge interest due to its non-toxicity and biodegradability. It also shows interesting anti-bacterial activity (Salama et al., 2020; Salama & Hesemann, 2020b), making it interesting for applications in the biomedical field. The amino group can be modified chemically in a variety of ways (Salama & Hesemann, 2018a), in view of the formation of biosourced polyelectrolytes (Salama, 2021). Chitosan therefore attracted considerable attention as a promising functional polysaccharide with tunable properties for several applications such as adsorption (Hassan et al., 2019; Monier et al., 2010), wound healing (Salama, 2018) and drug release (Costa-Pinto et al., 2009). Chitosan and its derivatives have been applied in various applications ranging from biomedical and pharmaceutical materials to environmental remediation. For electrochemical applications, chitosan has successfully been exploited to develop electrolytes and electrodes. These

materials have also attracted high interest due to their low cost, biodegradability, and environmental safety (Roy et al., 2021). When protonated, chitosan's physico-chemical properties are strongly modified, and cationic chitosan is capable of binding anionic compounds via ion exchange. In this context, the functionalization of chitosan with guanidine/guanidinium groups can bring significant benefits compared to the presence of the classical amine/ammonium chitosan. Promising trials were carried out for preparing guanidinylated chitosan derivatives for enhancing the antimicrobial properties and catalysis (Maleki et al., 2018; Sahariah et al., 2015). We already reported guanylation of chitosan following a simple strategy starting from parent chitosan and cyanamide, using scandium triflate as catalyst. The basicity of the guanidine group is several orders of magnitude higher compared to the one of the ammonium groups ( $pK_a$  guanidine = 13.6 vs.  $pK_a$  ammonia = 9.24). The basicity of guanidines further increases by substitution with alkyl groups (Eckert-Maksić et al., 2008). Guanidines therefore exists in aqueous solution nearly exclusively in their protonated, *i.e.*, the guanidinium form.

Dielectric spectroscopy is a technique that allows observing rotational molecular motions by probing the dipolar fluctuations. It is a valuable technique for the investigation of polymeric materials and in particular of polysaccharides (Einfeldt et al., 2001; Mohamed et al., 2020). Polyelectrolytes have attracted tremendous attention in the last decade for their ion-conducting properties (Bocharova & Sokolov, 2020; Ngai et al., 2016). High attention was paid to these materials for their potential in technologies such as energy storage (in batteries)(Cheng et al., 2018; Hallinan & Balsara, 2013), energy conversion (e.g., fuel cells) (Lu et al., 2008; Wang et al., 2011), electrochromic devices (Leones et al., 2017; Thakur et al., 2012), etc. In polyelectrolytes and poly(ionic liquid)s, the physico-chemical properties depend both on the cation and anion in the conductive material which can be altered or modified by ion exchange or by modulating the nature of substituents on the cation. In this way, the presence of specific groups on the cation or on the anion is able to impart highly specific properties to these systems (Anderson et al., 2005; Fei et al., 2004).

The current work investigates the influence of the functionalization of chitosan derivatives on their dielectric properties. More specifically, we studied the impact of the nature of the counter anion of guanylated chitosan on their dielectric properties at variable

temperature, in order to clarify the dynamic behavior of guanidinium groups and the counter anions. First, the guanylated chitosan derivatives, GChAc and GChCl were synthesized and characterized. The effect of the guanidinium groups and the counter anion as a function in electrical conductivity was studied.

## **2. Experimental part**

### **2.1. Synthesis of GChAc and GChCl**

The syntheses of chitosan derivatives (GChAc) and (GChCl) was accomplished by dissolving 2 g medium molecular weight chitosan (degree of deacetylation, 75–85%, Sigma-Aldrich) in 100 mL either 2 % acetic acid, or 2 % hydrochloric acid, respectively. Then 0.84 g cyanamide and 0.3 g scandium(III) triflate were added for each solution with continuous stirring at 100 °C for 48 h. The resulting mixtures were poured in acetone and the precipitated products were washed several times with acetone. N-guanidinium chitosan acetate (GChAc) and N-guanidinium chitosan chloride (GChCl) freeze-dried and obtained light brown solids.

### **2.3. Characterization methods**

<sup>13</sup>C Cross-Polarization Magic Angle Spinning (CP-MAS) experiments were carried out on a Varian VNMRs 400 MHz solid spectrometer by means of a two-channel probe with 7.5 mm ZrO<sub>2</sub> rotors. The attenuated total reflectance Fourier transform infrared (ATR FTIR) spectra of the chitosan, GChAc and GChCl were measured through a Thermo Nicolet FT-IR Avatar 320 with a diamond crystal. Spectra were documented from 500 to 4000 cm<sup>-1</sup>. TGA experiments were measured with a NETZSCH STA 409 PC device at a heating rate of 5 °C/min.

#### **2.3.4. Dielectric measurements**

The dielectric measurements were performed on discs of Ch, GChAc and GChCl of 2 mm thickness and 10 mm in diameter using broadband dielectric spectroscopy (BDS) employing an Alpha-A machine from novocontrol covering wide ranges of frequency (10<sup>1</sup> Hz - 10<sup>7</sup> Hz) and temperature (223 K to 423 K), connecting to a Quatro temperature controller system.

### 3. Results and Discussion

#### 3.1. Characterization of chitosan derivatives

Scandium (III) triflate has been applied as Lewis acid catalyst during the preparation of guanidinium group through the reaction between primary amines and cyanamide (Tsubokura et al., 2014). In the current study, two chitosan derivatives containing guanidinium groups have been produced from aqueous medium at 100 °C. The synthesis of guanidinium functions was proved using various techniques. Elemental analysis for Ch, GChAc and GChCl were calculated. The results show nitrogen content increasing from 7.7 % for neat Ch to reach 11.1 % and 12.3 % for GChAc and GChCl, respectively, indicating significant guanylation chitosan.

The suggested chemical structure and  $^{13}\text{C}$  CP-MAS solid state NMR of the two cationic chitosan derivatives are displayed in figure 1. The chitosan backbone structure principally gives rise to the signals in the range between 55–110 ppm, due to the carbon centers of the anhydroglucose units in this material labeled from 1 to 8 (Figure 1). The cationic chitosan derivatives show additional signals due to the presence of the newly formed guanidinium groups. GChAc shows new signal at 160 ppm (C9) which mentions to the created guanidinium groups. Additionally, the observed signal at 180 ppm may refer to the presence of acetate counter ions, as the guanylation process was carried out in acetic acid solution. Similarly, GChCl shows a new signal at 160 ppm (C9) which refers to the newly formed guanidinium groups.

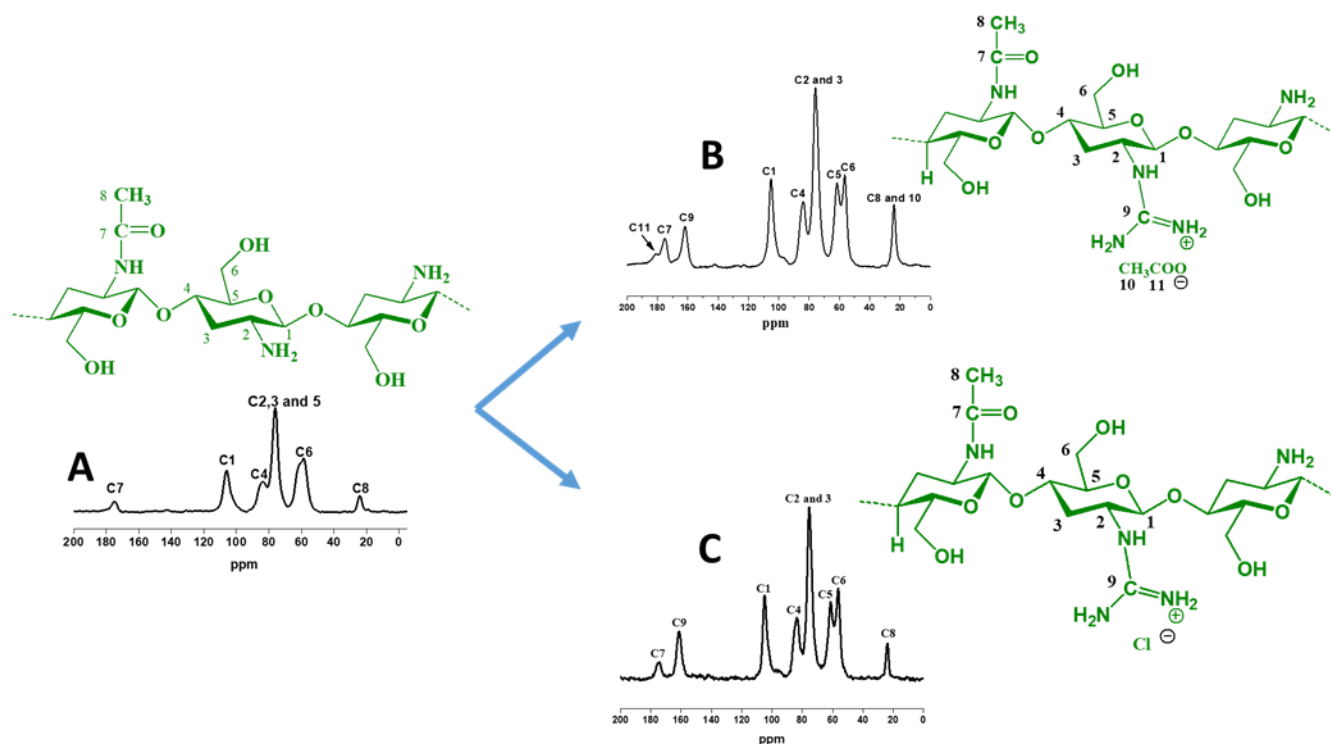


**Figure 1:** Chemical structures and solid state  $^{13}\text{C}$  CP-MAS NMR spectra of Ch (A), GChAc (B) and GChCl (C).

The presence of the various functional groups of chitosan and the two cationic derivatives was proved via by FT-IR spectroscopy (Figure 2). The spectrum of chitosan (A) shows the characteristic bands of chitosan backbone as previously described (Salama & Hesemann, 2018b). The higher intensity of the adsorption band at  $1629\text{ cm}^{-1}$  detected in the spectrum of the guanidinium derivatives B and C can be attributed to the generation of guanidinium moieties.

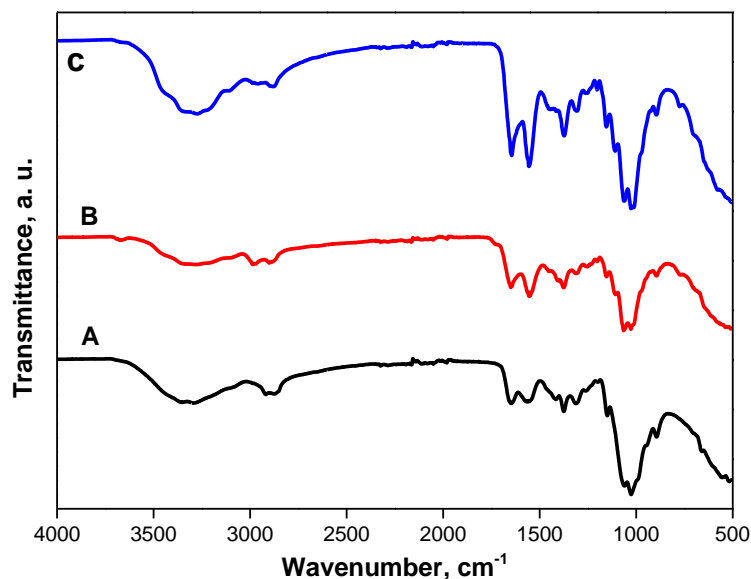


**Figure 2:** FT-IR spectra of Ch (A), GChAc (B) and GChCl (C).

The thermogravimetric analysis (TGA) thermograms for neat chitosan and the two cationic derivatives are displayed in Figure 3 (1). The weight loss of chitosan and the two derivatives divided to three regions, considered as I, II and III. At the first region (region I), the weight loss ranging from 1.3%–6.9% can be attributed to the loss of physically adsorbed water. N-guanidinium chitosan acetate contains high amount of water, compared to N-guanidinium chitosan chloride, which reflect the hydrophilicity of acetate anion. In the second region, N-guanidinium chitosan chloride starts to decompose at lower temperatures compared to N-guanidinium chitosan acetate and neat chitosan. The degradation pattern recorded 20% weight loss at 279 °C for chitosan and N-guanidinium chitosan acetate and at 250 °C for N-guanidinium chitosan chloride. The high thermal stability of ch and GChAc may result from the intramolecular and intermolecular hydrogen bonds that are affected by the chloride introduction. The third weight loss, region III, documented a high stability for the two cationic derivatives comparing to neat chitosan. The complete degradation was reached at 730, 680, 660 °C for N-guanidinium chitosan chloride, N-guanidinium chitosan acetate and chitosan, respectively.



The differential scanning calorimetry (DSC) thermograms of Ch, GChAc and GChCl are presented in figure 3(2). It can be seen that all the thermograms display two prominent peaks. The endothermic peaks observed between 70 and 90 °C can be associated to the loss of water (Chowdhury et al., 2022). The exothermic peaks at 295 °C for neat chitosan, 331 °C for GChAc and 317 °C for GChCl can be related to a thermal decomposition of amine units in chitosan and guanidinium groups in the chitosan derivatives. In agreement with TGA results, these results prove that the new guanylated chitosan derivatives exhibit slightly higher thermal stability.

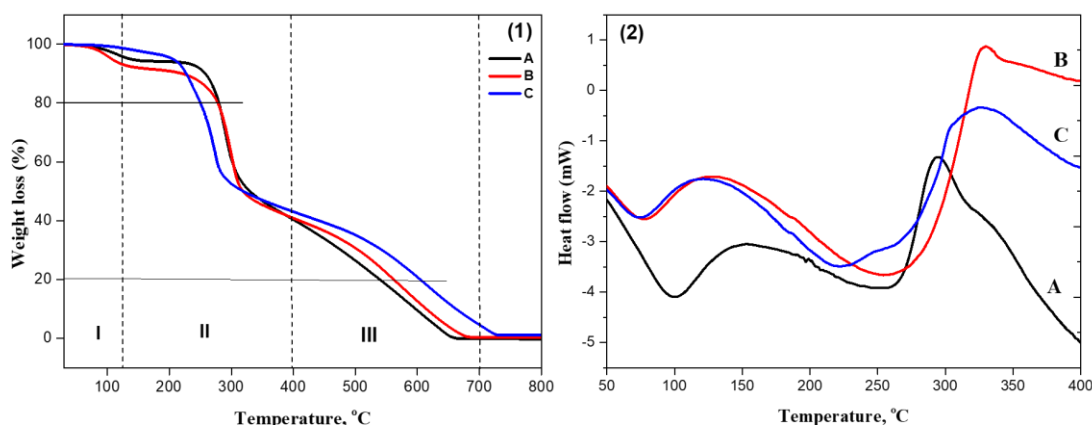


**Figure 3:** Thermogravimetric analyses (1) and DSC curves (2) of Ch (A), GChAc (B) and GChCl (C).

Finally, the morphologies and textures of the two cationic chitosan derivatives were examined via scanning electron microscopy (SEM) and transmission electron microscopy (TEM). Both materials show a relatively similar morphology as displayed by the two SEM images in Figure 4 A and B and present a rough surface with a certain porosity on the nanometric scale. Transmission electron microscopy (TEM) images (figure 4 C/D) also indicate relatively similar textures of agglomerated particles of a diameter of ~ 50 nm.

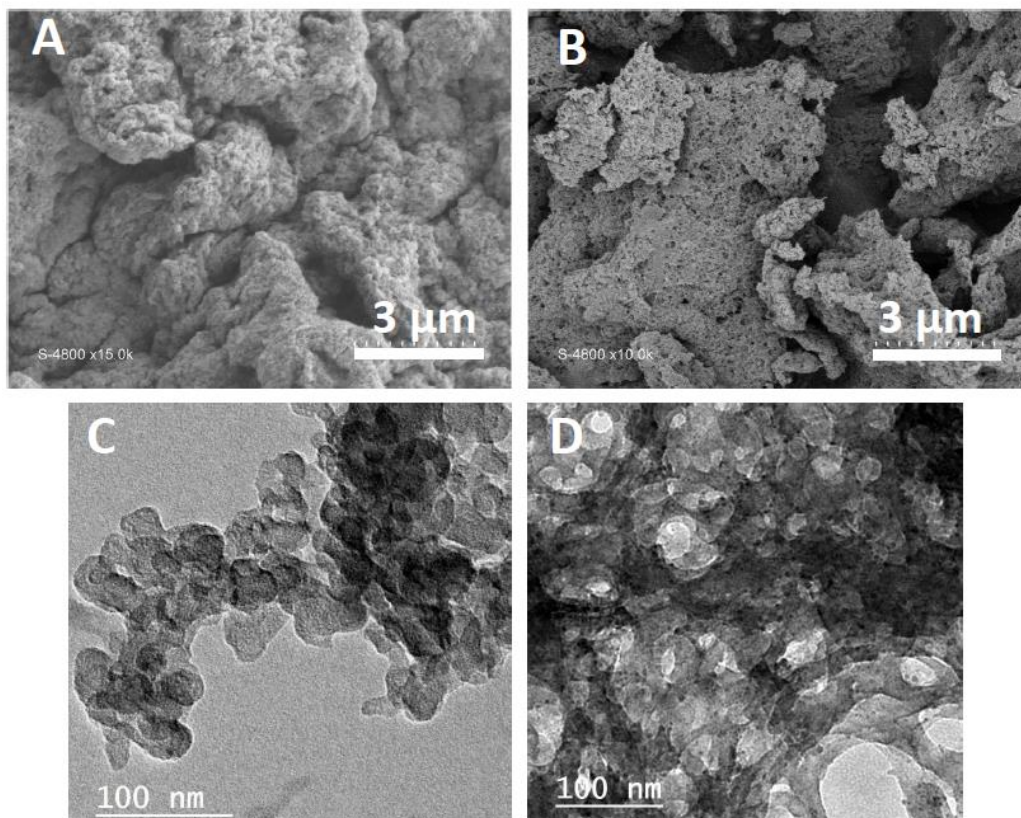


**Figure 4:** SEM and TEM images of GChAc (A and C) and GChCl (B and D), respectively.

### 3.2. Electrical properties

The electrical properties of the materials were investigated via broadband dielectric spectroscopy (BDS). In particular, we studied the three complex functions dielectric,  $\epsilon^*$ , conductivity  $\sigma^*$ , and modulus functions,  $M^*$ . Although they are equivalent, they are often utilized to emphasize different features of the underlying mechanisms of charge carriers' transport and molecular relaxations. In the case of charge bearing systems at sufficiently low frequencies, cooperative ion hopping dominantly affects the dielectric spectra in the complex permittivity  $\epsilon^*(\omega) = \epsilon'(\omega) - i\epsilon''(\omega)$ ; or in the complex conductivity;  $\sigma^*(\omega) = \sigma'(\omega) + i\sigma''(\omega)$ . Therefore, the dielectric storage ( $\epsilon'$ ), dielectric loss ( $\epsilon''$ ), electric loss modulus ( $M''$ ) as well as *ac* conductivity ( $\sigma_{ac}$ ) and *dc* conductivity ( $\sigma_{dc}$ ) for the systems under considerations are investigated over wide frequency and temperature ranges.

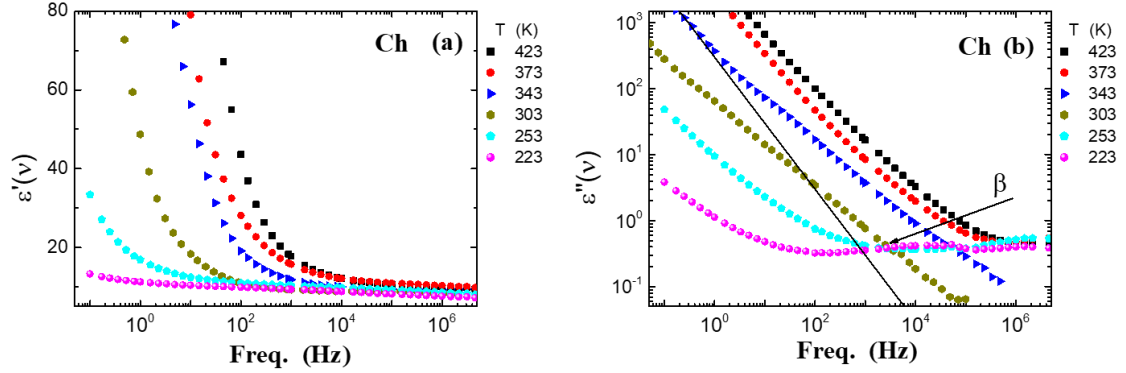


**Figure 5.** Dielectric storage (a) and dielectric loss (b) of chitosan (Ch) measured at variable temperatures

Figure 5 a and b display  $\epsilon'$  and loss  $\epsilon''$  spectra of the Ch at different temperatures. From Figure 5a, it can be seen that  $\epsilon'$  is approximately frequency independent at low temperature ( $T = 223$  K), while it shows frequency dependence at higher temperatures ( $T > 223$  K). At high frequencies, it slightly depends on the frequency, which is translated to a relaxation peak in the loss  $\epsilon''$  spectra, *cf.* Fig 5b. This is due to the lag of molecules behind the alternation of the electric field at higher frequency. At low frequencies, the  $\epsilon'$  greatly increases. This is related to the well-known phenomenon that is the electrode polarization (Kremer & Schönhal, 2003).

In the dielectric loss  $\epsilon''$  and at low temperature ( $T \leq 303$  K), a relaxation  $\beta$ -process is observed. The process originates from some local motion in the Ch chain, which is slowed down upon cooling. In polysaccharides, two secondary relaxation processes of different molecular origin were reported (Cerveny et al., 2008; Kaminski et al., 2008; Salama et al., 2021). One secondary relaxation process is of cooperative molecular nature as large parts of molecule take part in the motion. This is generally referred to as Johari-Goldstein (JG-) relaxations, which aroused from the motions of all parts of the polymer segments. This process is not analyzed here since it is masked by the conductivity contribution. The conductivity contribution is given by a line of  $\epsilon''(\omega) \approx \frac{\sigma'}{\epsilon_0 \omega}$  which is included in Fig 5b (Mohamed et al., 2020). The other secondary relaxation ( $\beta$ -relaxation) originates from the local motions within the chains of polysaccharides.

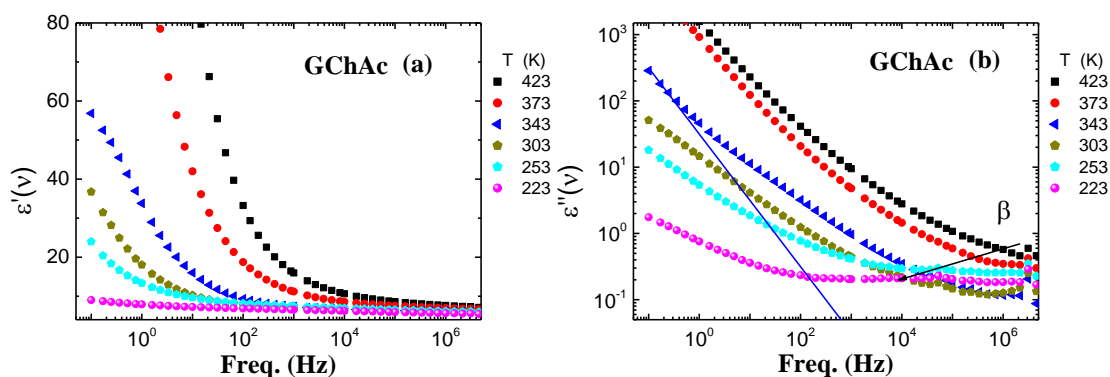


**Figure 6.** Dielectric storage (a) and dielectric loss (b) of GChAc measured at different temperatures.

In the case of N-guanidinium chitosan acetate GChAc, the dielectric storage and loss are depicted in figure 6a and b, respectively. Here, the  $\epsilon'$  is smaller compared to the case of Ch (figure 5a). The  $\beta$ -process is again observed at  $T \leq 253$  K. However, the process is smaller in its height, see below.

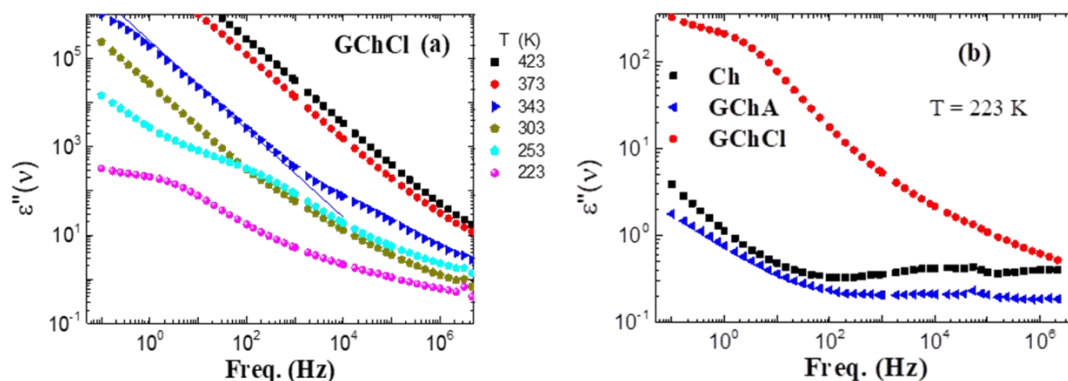


**Figure 7.** (a) Dielectric loss of GChCl measured at temperature as indicated. (b) dielectric loss of Ch, GChAc, and GChCl compared at the  $T = 223$  K.

For N-guanidinium chitosan chloride (GChCl), the  $\epsilon''$  is illustrated in figure 7a. It is completely altered. The  $\beta$ -process is depleted. The  $\epsilon''$  spectra mimics that of conductive materials. This means that the presence of chloride counter anions attached to N-guanidinium chitosan backbone covers the fluctuations along the N-guanidinium chitosan segments. A comparison between the dielectric loss of all systems at  $T = 223\text{K}$  is displayed in figure 7b. It can clearly be seen that the strength of the  $\beta$ -process is somewhat smaller in the case of GChAc compared to the case of Ch, while it is completely depleted in the case of GChCl, *i.e.*, the ion motion dominates the spectra and masks any process due to the molecular relaxation.

In the modulus presentation, which reads

$$M^* = M' + i M'' = 1/\epsilon^* = i\omega\epsilon_0/\sigma^* \quad (1)$$

with  $\epsilon_0$  is the permittivity of free space, two maxima are observed in the cases of Ch and GChAc (figure 8a and b) at  $T < 303\text{ K}$ . The maxima seen in the case of GChAc is broader compared to the case of Ch. For clarity, one modulus spectrum at  $T = 423\text{K}$  for Ch is also included in figure 8b. In the case of GChCl only one maximum can be recognized (figure 8c). This peak maximum denotes the conductivity relaxation  $\sigma$ -process (Kremer & Schönhals, 2003; Viciosa et al., 2004). This process was widely investigated and revealed to be associated with the hopping motion of ions in the disordered structure and correlated to the dc conductivity (see below)(González-Campos et al., 2009; Meißner et al., 2000). For all cases and by picking up the frequency position of this maximum  $f_0$ , this process is faster in the case of GChCl compared to the other cases reported here (see Figure 8d), *i.e.*, this process is controlled by the presence of more mobile ions in the case of GChCl.

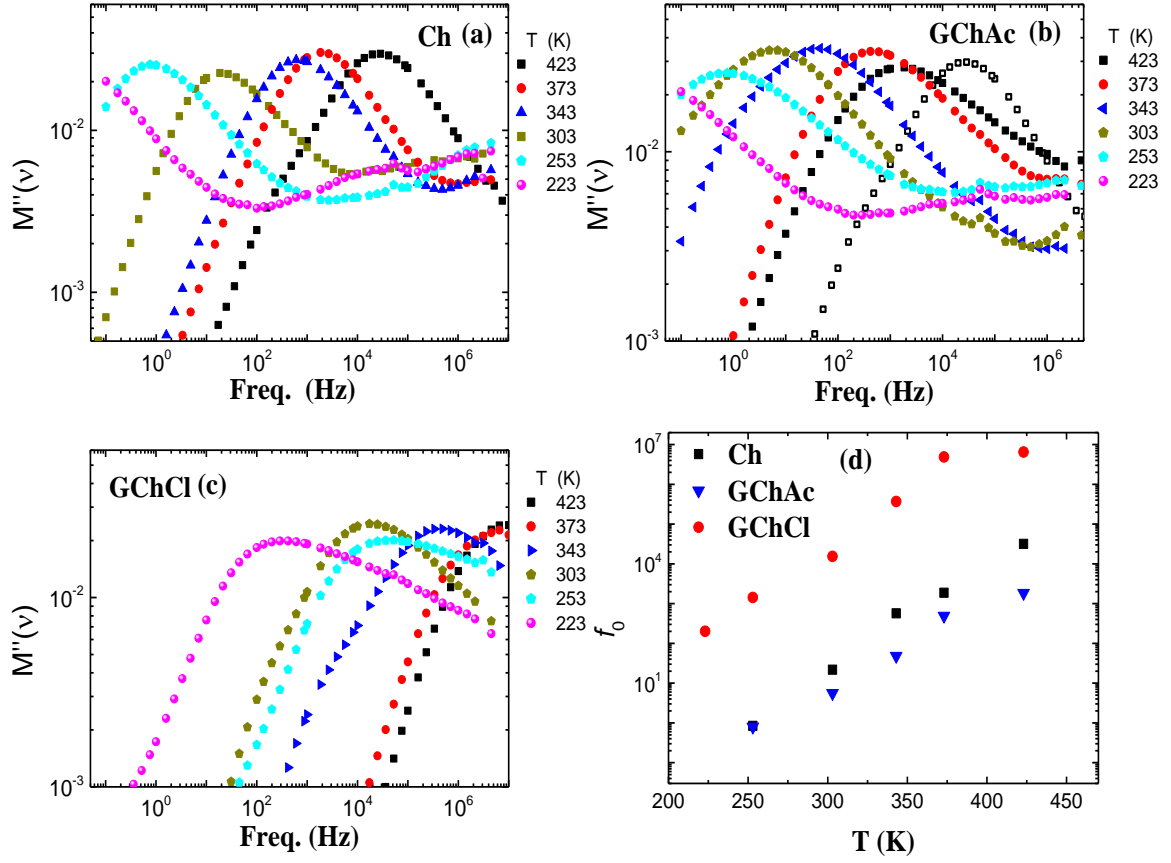


**Figure 8.** Dielectric modulus  $M''(\nu)$  of chitosan Ch (a), GChAc (b) and GChCl (c) at different temperatures. (d) peak maximum positions of the  $\sigma$  process.

The investigation of *ac* conductivity ( $\sigma_{ac}$ ) is an essential for exploring the electrical conduction of a system upon employing an electrical field (Tan et al., 2016). The conductivity depends both on the density and the mobility of free charge carriers, *i.e.*, it increases with mobility and density of free charge carriers (Griffin et al., 2014; Jlassi et al., 2017; Sangoro et al., 2009).

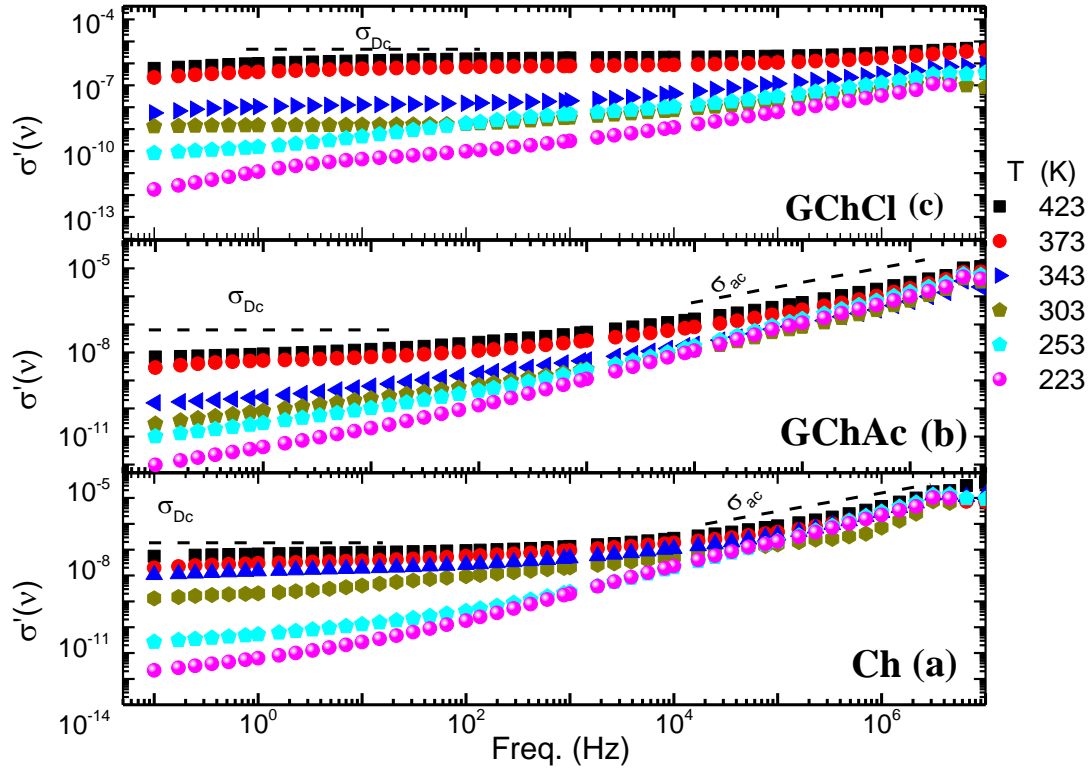


**Figure 9.** The real part of conductivity  $\sigma'(\nu)$  of chitosan Ch (a), GChAc (b) and GChCl (c) measured at temperature as indicated.

For all cases, the real part of the conductivity  $\sigma'(\nu)$  as a function of frequency is displayed in figure 9. Two different power-law regimes are recognized following the power-law of Jonscher (Jonscher, 1981),

$$\sigma_{ac}(\omega) = \sigma_{Dc} + A\omega^s \quad (2)$$

with  $\sigma_{Dc}$  and  $A$  are the Dc conductivity, and the pre-exponential factor, respectively. The latter depends on temperature and material. Jonscher's exponent  $s$  correlates the degree of interaction between mobile ions with the lattices (Jonscher, 1981). In regime  $\sigma_{Dc}$ , there is no change with frequency (frequency independent), which dominates the low frequency regime. Our results indicate that in the case of GChCl, the  $\sigma_{Dc}$  is 4 orders of magnitude higher compared to Ch and GChAc. The  $\sigma_{Dc}(T)$  for Ch, GChAc and GChCl

derivatives were determined and added to Figure 10 which shows the temperature dependence of the Dc conductivity,  $\sigma_{Dc}$ . The  $\sigma_{Dc}(T)$  follows Arrhenius law, which reads,

$$\sigma_{Dc} = \sigma_{\infty} \exp\left(\frac{-E_a}{k_B T}\right) \quad (3)$$

where  $\sigma_{\infty}$  and  $k_B$  are the conductivity at infinite temperatures and Boltzmann constant, respectively. The  $E_a$  is the activation energy. The fitting parameters are summarized in table 1.

**Table 1.** Parameters used to fit using Eq.3

System	$E_a$ [kJ/mol]	$\sigma_{\infty}$ [S/cm]
Ch	47	$2.4 \times 10^{-2}$
GChAc	56	$2.2 \times 10^{-2}$
GChCl	52	$0.25 \times 10^{-2}$

As already mentioned, the Dc conductivity is proportional to the density of the charge carriers and their mobility. According to the Stokes–Einstein equation, the mobility is inversely related to the viscosity. Since the ratio of  $\sigma_{Dc}$  of GChCl to that of Ch at the same temperature increases, and if the viscosity is similar in the two cases, we can conclude that the number density of the charge carrier increases significantly. On the other side, the ratio of  $\sigma_{dc}$  of GChAc to that of Ch decreases. Assuming again that the viscosity is similar, this would indicate an increase in the dynamic's radius (Rössler, 1990) or a decrease of the mobility of the charge carriers in the GChAc material. This phenomenon can certainly be attributed to strong hydrogen bonding between the guanidinium acetate backbone and the acetate counter ions, resulting in its significantly lower mobility. The interaction strength of the counterions with the Ch main chain may therefore give interesting insights in the dynamics of the counter-anions. The interactions of chloride anions with the guanylated chitosan backbone are weaker compared to those of acetate. Therefore, chloride resides shorter time on the main chain than acetate. For the same reason, the concentration of ‘free’ chloride should be higher than that of acetate, resulting in a higher conductivity.



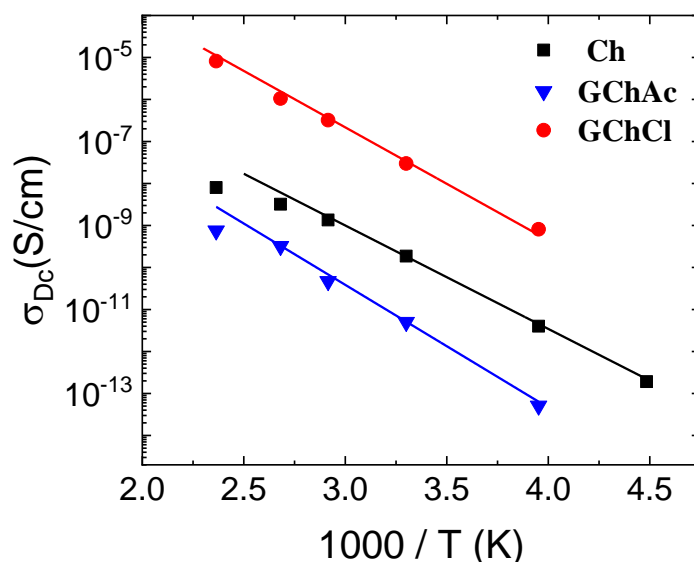


**Figure 10.** Dc conductivity  $\sigma_{Dc}$  (v) vs. temperature of chitosan Ch, GChAc and GChCl.

#### 4. Conclusion

New chitosan-based guanidinium derivative, i.e., GChAc and GChCl, were prepared and thoroughly characterized. In particular, we focused here on the investigation of the dielectric properties of chitosan and its derivatives via dielectric measurements. In chitosan and GChAc, two relaxation processes were identified, whereas no relaxation processes could be identified in GChCl. Compared to chitosan, the electrical conductivity of GChCl is four orders of magnitude higher due to both higher ion mobility and higher number of ions conducting species. On the opposite, the conductivity of GChAc is lower compared to neat chitosan. We attribute this result to the increase in the dynamic's radius or the decrease of the mobility of the charge carriers. In conclusion, we report new biodegradable and sustainable polymer electrolyte with controllable conductivity, and we believe that these systems give interesting insight in ion conduction phenomena in these systems that have high potential for the construction of “green” technological applications.

**Declaration of competing interest:**

The author declares no competing financial interest

**References**

- Anderson, J. L., Ding, R., Ellern, A., & Armstrong, D. W. (2005). Structure and Properties of High Stability Geminal Dicationic Ionic Liquids. *Journal of the American Chemical Society*, 127(2), 593–604. <https://doi.org/10.1021/ja046521u>
- Bocharova, V., & Sokolov, A. P. (2020). Perspectives for Polymer Electrolytes: A View from Fundamentals of Ionic Conductivity. *Macromolecules*, 53(11), 4141–4157. <https://doi.org/10.1021/acs.macromol.9b02742>
- Cervený, S., Alegría, Á., & Colmenero, J. (2008). Broadband dielectric investigation on poly(vinyl pyrrolidone) and its water mixtures. *The Journal of Chemical Physics*, 128(4), 044901. <https://doi.org/10.1063/1.2822332>
- Cheng, X., Pan, J., Zhao, Y., Liao, M., & Peng, H. (2018). Gel Polymer Electrolytes for Electrochemical Energy Storage. *Advanced Energy Materials*, 8(7), 1702184. <https://doi.org/10.1002/aenm.201702184>
- Chowdhury, F., Ahmed, S., Rahman, M., Ahmed, M. A., Hossain, M. D., Reza, H. M., Park, S. Y., & Sharker, S. M. (2022). Chronic wound-dressing chitosan-polyphenolic patch for pH responsive local antibacterial activity. *Materials Today Communications*, 31, 103310. <https://doi.org/10.1016/j.mtcomm.2022.103310>
- Costa-Pinto, A. R., Correlo, V. M., Sol, P. C., Bhattacharya, M., Charbord, P., Delorme, B., Reis, R. L., & Neves, N. M. (2009). Osteogenic differentiation of human bone marrow mesenchymal stem cells seeded on melt based chitosan scaffolds for bone tissue engineering applications. *Biomacromolecules*, 10(8), 2067–2073. <https://doi.org/10.1021/bm9000102>
- Eckert-Maksić, M., Glasovac, Z., Trošelj, P., Kütt, A., Rodima, T., Koppel, I., & Koppel, I. A. (2008). Basicity of Guanidines with Heteroalkyl Side Chains in Acetonitrile. *European Journal of Organic Chemistry*, 2008(30), 5176–5184. <https://doi.org/10.1002/ejoc.200800673>
- Einfeldt, J., Meißner, D., & Kwasniewski, A. (2001). Polymerdynamics of cellulose and other polysaccharides in solid state-secondary dielectric relaxation processes. *Progress in Polymer Science*, 26(9), 1419–1472. [https://doi.org/10.1016/S0079-6700\(01\)00020-X](https://doi.org/10.1016/S0079-6700(01)00020-X)
- Fei, Z., Zhao, D., Geldbach, T. J., Scopelliti, R., & Dyson, P. J. (2004). Brønsted Acidic Ionic Liquids and Their Zwitterions: Synthesis, Characterization and pKa Determination. *Chemistry - A European Journal*, 10(19), 4886–4893. <https://doi.org/10.1002/chem.200400145>
- González-Campos, J. B., Prokhorov, E., Luna-Bárcenas, G., Fonseca-García, A., & Sanchez, I. C. (2009). Dielectric relaxations of chitosan: The effect of water on the  $\alpha$ -relaxation and the glass transition temperature. *Journal of Polymer Science Part B: Polymer Physics*, 47(22), 2259–2271. <https://doi.org/10.1002/polb.21823>
- Griffin, P. J., Cosby, T., Holt, A. P., Benson, R. S., & Sangoro, J. R. (2014). Charge Transport and Structural Dynamics in Carboxylic-Acid-Based Deep Eutectic Mixtures. *The Journal of Physical Chemistry B*, 118(31), 9378–9385.

- <https://doi.org/10.1021/jp503105g>
- Hallinan, D. T., & Balsara, N. P. (2013). Polymer Electrolytes. *Annual Review of Materials Research*, 43(1), 503–525. <https://doi.org/10.1146/annurev-matsci-071312-121705>
- Hassan, H., Salama, A., El-ziaty, A. K., & El-sakhawy, M. (2019). New chitosan / silica / zinc oxide nanocomposite as adsorbent for dye removal. *International Journal of Biological Macromolecules*, 131, 520–526. <https://doi.org/10.1016/j.ijbiomac.2019.03.087>
- Jlassi, I., Sdiri, N., & Elhouichet, H. (2017). Electrical conductivity and dielectric properties of MgO doped lithium phosphate glasses. *Journal of Non-Crystalline Solids*, 466–467, 45–51. <https://doi.org/10.1016/j.jnoncrysol.2017.03.042>
- Jonscher, A. K. (1981). A new understanding of the dielectric relaxation of solids. *Journal of Materials Science*, 16(8), 2037–2060. <https://doi.org/10.1007/BF00542364>
- Kaminski, K., Kaminska, E., Hensel-Bielowka, S., Chelmecka, E., Paluch, M., Ziolo, J., Wlodarczyk, P., & Ngai, K. L. (2008). Identification of the Molecular Motions Responsible for the Slower Secondary ( $\beta$ ) Relaxation in Sucrose. *The Journal of Physical Chemistry B*, 112(25), 7662–7668. <https://doi.org/10.1021/jp711502a>
- Kremer, F., & Schönhal, A. (2003). *Broadband Dielectric Spectroscopy* (F. Kremer & A. Schönhal (eds.)). Springer Berlin Heidelberg. <https://doi.org/10.1007/978-3-642-56120-7>
- Le Bras, D., Strømme, M., & Mihranyan, A. (2015). Characterization of Dielectric Properties of Nanocellulose from Wood and Algae for Electrical Insulator Applications. *The Journal of Physical Chemistry B*, 119(18), 5911–5917. <https://doi.org/10.1021/acs.jpccb.5b00715>
- Leones, R., Sabadini, R. C., Sentanin, F. C., Esperança, J. M. S. S., Pawlicka, A., & Silva, M. M. (2017). Polymer electrolytes for electrochromic devices through solvent casting and sol-gel routes. *Solar Energy Materials and Solar Cells*, 169, 98–106. <https://doi.org/10.1016/j.solmat.2017.04.047>
- Lu, S., Pan, J., Huang, A., Zhuang, L., & Lu, J. (2008). Alkaline polymer electrolyte fuel cells completely free from noble metal catalysts. *Proceedings of the National Academy of Sciences*, 105(52), 20611–20614. <https://doi.org/10.1073/pnas.0810041106>
- Maleki, A., Firouzi-Haji, R., & Hajizadeh, Z. (2018). Magnetic guanidinylated chitosan nanobiocomposite: A green catalyst for the synthesis of 1,4-dihydropyridines. *International Journal of Biological Macromolecules*, 116, 320–326. <https://doi.org/10.1016/j.ijbiomac.2018.05.035>
- Meißner, D., Einfeldt, J., & Kwasniewski, A. (2000). Contributions to the molecular origin of the dielectric relaxation processes in polysaccharides – the low temperature range. *Journal of Non-Crystalline Solids*, 275(3), 199–209. [https://doi.org/10.1016/S0022-3093\(00\)00248-9](https://doi.org/10.1016/S0022-3093(00)00248-9)
- Mohamed, F., Hameed, T. A., Abdelghany, A. M., & Turkey, G. (2020). Structure–dynamic properties relationships in poly(ethylene oxide)/silicon dioxide nanocomposites: dielectric relaxation study. *Polymer Bulletin*. <https://doi.org/10.1007/s00289-020-03368-0>
- Monier, M., Ayad, D. M., Wei, Y., & Sarhan, A. A. (2010). Adsorption of Cu(II),

- Co(II), and Ni(II) ions by modified magnetic chitosan chelating resin. *Journal of Hazardous Materials*, 177(1–3), 962–970.  
<https://doi.org/10.1016/j.jhazmat.2010.01.012>
- Ngai, K. S., Ramesh, S., Ramesh, K., & Juan, J. C. (2016). A review of polymer electrolytes: fundamental, approaches and applications. *Ionics*, 22(8), 1259–1279.  
<https://doi.org/10.1007/s11581-016-1756-4>
- Rössler, E. (1990). Indications for a change of diffusion mechanism in supercooled liquids. *Physical Review Letters*, 65(13), 1595–1598.  
<https://doi.org/10.1103/PhysRevLett.65.1595>
- Roy, B. K., Tahmid, I., & Rashid, T. U. (2021). Chitosan-based materials for supercapacitor applications: a review. *Journal of Materials Chemistry A*, 9(33), 17592–17642. <https://doi.org/10.1039/D1TA02997E>
- Sahariah, P., Óskarsson, B. M., Hjálmarsson, M. Á., & Másson, M. (2015). Synthesis of guanidinylated chitosan with the aid of multiple protecting groups and investigation of antibacterial activity. *Carbohydrate Polymers*, 127, 407–417.  
<https://doi.org/10.1016/j.carbpol.2015.03.061>
- Salama, A. (2018). Chitosan based hydrogel assisted spongelike calcium phosphate mineralization for in-vitro BSA release. *International Journal of Biological Macromolecules*, 108, 471–476. <https://doi.org/10.1016/j.ijbiomac.2017.12.035>
- Salama, A. (2021). Recent progress in preparation and applications of chitosan / calcium phosphate composite materials. *International Journal of Biological Macromolecules*, 178, 240–252. <https://doi.org/10.1016/j.ijbiomac.2021.02.143>
- Salama, A., & El-Sakhawy, M. (2014). Preparation of polyelectrolyte/calcium phosphate hybrids for drug delivery application. *Carbohydrate Polymers*, 113, 500–506. <https://doi.org/10.1016/j.carbpol.2014.07.022>
- Salama, A., Hasanin, M., & Hesemann, P. (2020). Synthesis and antimicrobial properties of new chitosan derivatives containing guanidinium groups. *Carbohydrate Polymers*, 241, 116363.  
<https://doi.org/10.1016/j.carbpol.2020.116363>
- Salama, A., & Hesemann, P. (2018a). New N-guanidinium chitosan/silica ionic microhybrids as efficient adsorbent for dye removal from waste water. *International Journal of Biological Macromolecules*, 111, 762–768.  
<https://doi.org/10.1016/j.ijbiomac.2018.01.049>
- Salama, A., & Hesemann, P. (2018b). Synthesis of N-Guanidinium-chitosan/silica hybrid composites: Efficient adsorbents for anionic pollutants. *Journal of Polymers and the Environment*, 26(5), 1986–1997.  
<https://doi.org/10.1007/s10924-017-1093-3>
- Salama, A., & Hesemann, P. (2020a). Recent Trends in Elaboration, Processing, and Derivatization of Cellulosic Materials Using Ionic Liquids. *ACS Sustainable Chemistry & Engineering*, 8, 17893–17907.  
<https://doi.org/10.1021/acssuschemeng.0c06913>
- Salama, A., & Hesemann, P. (2020b). Synthesis and characterization of N - guanidinium chitosan / silica ionic hybrids as templates for calcium phosphate mineralization. *International Journal of Biological Macromolecules*, 147, 276–283. <https://doi.org/10.1016/j.ijbiomac.2020.01.046>
- Salama, A., Mohamed, F., & Hesemann, P. (2021). Preparation and dielectric

- relaxation of a novel ionocellulose derivative. *Carbohydrate Polymer Technologies and Applications*, 2, 100087.  
<https://doi.org/10.1016/j.carpta.2021.100087>
- Salama, A., Shoueir, K. R., & Aljohani, H. A. (2017). Preparation of sustainable nanocomposite as new adsorbent for dyes removal. *Fibers and Polymers*, 18(9), 1825–1830. <https://doi.org/10.1007/s12221-017-7396-0>
- Sangoro, J. R., Turkey, G., Abdel Rehim, M., Iacob, C., Naumov, S., Ghoneim, A., Kärger, J., & Kremer, F. (2009). Charge Transport and Dipolar Relaxations in Hyperbranched Polyamide Amines. *Macromolecules*, 42(5), 1648–1651.  
<https://doi.org/10.1021/ma8024046>
- Tan, F. K., Hassan, J., Wahab, Z. A., & Azis, R. S. (2016). Electrical conductivity and dielectric behaviour of manganese and vanadium mixed oxide prepared by conventional solid state method. *Engineering Science and Technology, an International Journal*, 19(4), 2081–2087.  
<https://doi.org/10.1016/j.jestch.2016.08.002>
- Thakur, V. K., Ding, G., Ma, J., Lee, P. S., & Lu, X. (2012). Hybrid Materials and Polymer Electrolytes for Electrochromic Device Applications. *Advanced Materials*, 24(30), 4071–4096. <https://doi.org/10.1002/adma.201200213>
- Tsubokura, K., Iwata, T., Taichi, M., Kurbangalieva, A., Fukase, K., Nakao, Y., & Tanaka, K. (2014). Direct guanylation of amino groups by cyanamide in water: Catalytic generation and activation of unsubstituted carbodiimide by scandium(iii) triflate. *Synlett*, 25(9), 1302–1306. <https://doi.org/10.1055/s-0033-1341080>
- Viciosa, M. T., Dionísio, M., Silva, R. M., Reis, R. L., & Mano, J. F. (2004). Molecular Motions in Chitosan Studied by Dielectric Relaxation Spectroscopy. *Biomacromolecules*, 5(5), 2073–2078. <https://doi.org/10.1021/bm049685b>
- Wang, Y., Chen, K. S., Mishler, J., Cho, S. C., & Adroher, X. C. (2011). A review of polymer electrolyte membrane fuel cells: Technology, applications, and needs on fundamental research. *Applied Energy*, 88(4), 981–1007.  
<https://doi.org/10.1016/j.apenergy.2010.09.030>
- Yin, Y., Zhang, C., Yu, W., Kang, G., Yang, Q., Shi, Z., & Xiong, C. (2020). Transparent and flexible cellulose dielectric films with high breakdown strength and energy density. *Energy Storage Materials*, 26, 105–111.  
<https://doi.org/10.1016/j.ensm.2019.12.034>